

Difference in evaporation residue yields in the cold and hot fusion reactions

Avazbek Nasirov^{1,2}, Giorgio Giardina^{3,4,5}, Giuseppe Mandaglio^{3,4,5},
Kyungil Kim⁶ and Youngman Kim⁶

¹BLTP, Joint Institute for Nuclear Research, Joliot-Curie 6, 141980 Dubna, Russia

²Institute of Nuclear Physics, Ulugbek, 100214, Tashkent, Uzbekistan

³Dipartimento di Fisica e di Scienze della Terra dell' Università di Messina, Salita Sperone 31, 98166 Messina, Italy

⁴Istituto Nazionale di Fisica Nucleare, Sezione di Catania, Italy

⁵Centro Siciliano di Fisica Nucleare e Struttura della Materia 95125 Catania, Italy

⁶Rare Isotope Science Project, Institute for Basic Science, Daejeon 305-811, Republic of Korea

E-mail: nasirov@jinr.ru

Abstract. An interest to study the mechanism of the complete fusion with massive nucleus reactions was caused by difficulties of synthesizing superheavy elements due to their small cross sections. Theoretical models used to obtain knowledge about fusion mechanism in heavy ion collisions at low energies are requested. We present the theoretical results of the compound nucleus (CN) formation and evaporation residue (ER) cross sections obtained for the $^{48}\text{Ca}+^{248}\text{Cm}$ and $^{58}\text{Fe}+^{232}\text{Th}$ reactions leading to the formation of CN with $A = 296$ and $A = 290$ of the superheavy element Lv ($Z = 116$), respectively. The ER cross sections, which can be measured directly, are determined by the complete fusion and survival probabilities of the heated and rotating CN. Those probabilities can not be measured unambiguously but the knowledge about them is important to study the formation mechanism of the observed products and to estimate the ER cross sections of the expected isotopes of elements. For this aim, the $^{48}\text{Ca}+^{249}\text{Cf}$ and $^{64}\text{Ni}+^{232}\text{Th}$ reactions are also considered. The survival probability of the heated and rotating CN is sensitive to the used mass and shell correction values of superheavy nuclei. The ER cross sections obtained by using the macroscopic-microscopic model with mass and fission barrier values calculated by Warsaw group lead to smaller ER values for all reactions in comparison with the case when the masses and shell correction calculated by P. Möller *et al* are used.

1. Introduction

In recent decades, interest in nuclear physics has increased due to observation of events in the synthesis of new superheavy elements (SHE) with the atomic numbers $Z = 114$ – 118 [1,2]. The achievements in hot fusion reactions led to the discovery of new elements Fl ($Z = 114$) and Lv ($Z = 116$) after those results have been confirmed in other similar experiments. Isotopes $^{286,287}\text{Fl}$ were obtained in the reaction ^{48}Ca with ^{242}Pu in an experiment at Berkeley gas-filled separator Lawrence National Laboratory (LBNL) [3] while isotopes $^{288-291}\text{Fl}$ were obtained in the bombing of ^{244}Pu with ^{48}Ca at the recoil separator TASCA experiment of GSI [4] in Darmstadt. Events corresponding to the synthesis of isotopes $^{292,293}\text{Lv}$ were observed in the $^{48}\text{Ca}+^{248}\text{Cm}$ reaction by the velocity filter SHIP at GSI [5]. Two reasons have contributed to



the success of the synthesis of superheavy elements with $Z = 113$ — 118 : 1) large cross sections of the compound nucleus formation for hot fusion reactions and 2) increase of the fission barrier as they approach to the island of stability [6,7] (see Fig. 1). As Fig. 1 shows, the synthesis cross sections of SHE with $Z = 104$ — 111 in cold fusion are sufficiently larger than ones obtained in the hot fusion reactions. Starting from SHE $Z = 112$ the ER cross sections measured in the hot fusion become larger. The possibility of cold fusion have been exhausted for the synthesis of SHE with $Z \geq 114$. Experimental results showed that the ER cross section (σ_{ER}) in cold fusion reactions fall sharply with increasing the electric charge of the formed compound nucleus [8] (see Fig. 1). The last SHE synthesized in cold fusion is $Z=113$, which was obtained at RIKEN (Japan) by using the $^{70}\text{Zn} + ^{209}\text{Bi}$ reaction. After repeated and prolonged experiments reached the lowest value σ_{ER} equal to 22 femtobarn (fb) [9], (1fb= 10^{-15} barn).

The name cold fusion is associated with a low value of the minimal excitation energy ($E_{\text{CN}}^* < 20$ MeV) of the compound nucleus. The smallness of the excitation energy $E_{\text{CN}}^* = E_{\text{c.m.}} + Q_{\text{gg}}$ follows from the large negative values of Q_{gg} , which is the reaction energy balance is: $Q_{\text{gg}} = B_1 + B_2 - B_{\text{CN}}$. The binding energies of the initial projectile and target nuclei (B_1 and B_2) are obtained from the mass tables in Ref. [10], while the one of CN (B_{CN}) is obtained from the theoretical mass tables [11,12]. The use of nuclear binding energies including shell effects in calculations of the potential energy surface (PES) (see Fig. 2) and driving potential U_{dr} of DNS lead to the appearance of hollows on the PES around the charge and mass values corresponding to the constituents of DNS with the magic proton or/and neutron numbers (see Figs. 3 and 4).

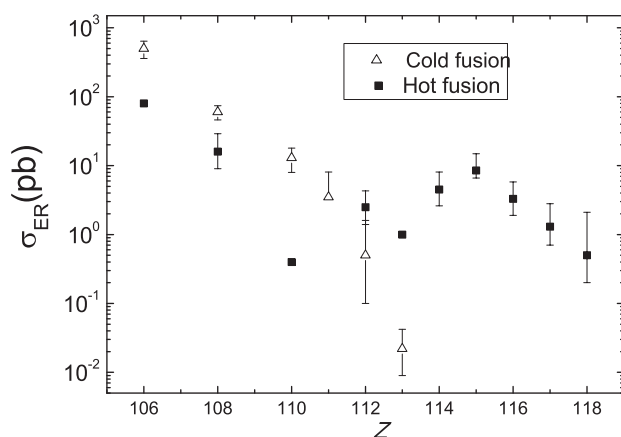


Figure 1. The maximum values of the excitation functions measured in synthesis of the superheavy elements (Z) in the cold (opening triangles) [8] and hot (full squares) fusion [1,2] reactions.

2. Outline of the approach

The ER formation process is the last stage of the reaction mechanism in heavy ion collisions at $E_{\text{c.m.}}$ energies near the Coulomb barrier:

$$\sigma_{\text{ER}}(E_{\text{CN}}^*) = \sigma_{\text{cap}}(E_{\text{c.m.}}) P_{\text{CN}}(E_{\text{DNS}}^*) W_{\text{sur}}(E_{\text{CN}}^*), \quad (1)$$

where $\sigma_{\text{cap}}(E_{\text{c.m.}})$ is the capture cross section, $P_{\text{CN}}(E_{\text{DNS}}^*)$ is the complete fusion probability and $W_{\text{sur}}(E_{\text{CN}}^*)$ is the survival probability of the heated and rotating CN against fission; $E_{\text{DNS}}^* = E_{\text{c.m.}} - V_{\text{min}}$ is the excitation energy of DNS which is determined by an amount of the dissipated part of the relative kinetic energy; V_{min} is the minimum of the potential well where DNS has been trapped at capture.

Our experience of calculations shows that the capture probability is larger for the hot fusion reactions because the size of the potential well is larger due to the weaker Coulomb repulsion

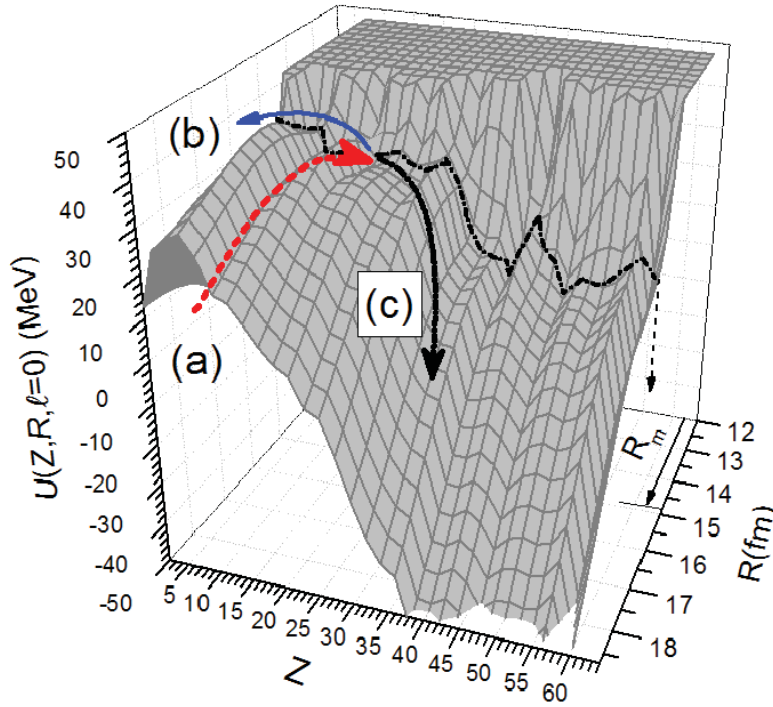


Figure 2. (Color online) Potential energy surface calculated for the DNS leading to formation of the $^{296}_{116}\text{CN}$ as a function of the relative distance between the centers of mass of interacting nuclei and charge number of a fragment. The capture stage path for the $^{48}\text{Ca} + ^{248}\text{Cm}$ reaction is shown by arrow (a) and complete fusion by multinucleon transfer occurs (b) if DNS overcomes intrinsic fusion barrier. Arrow (c) shows one of possibilities of DNS decay into two fragments without reaching complete fusion stage (quasifission process). The broken dot-dashed line corresponds to the driving potential $U(Z, R_m)$ which is determined by the minimum values of the potential wells for each charge value Z . R_m is the position of the minimum value of interaction potential on the relative distance R .

in comparison with the one in cold fusion reaction: $(Z_1 \times Z_2)_{\text{hot}} < (Z_1 \times Z_2)_{\text{cold}}$ since the hot fusion reactants are more charge asymmetric than the ones of cold fusion.

A huge hindrance to transformation of the DNS, which is formed at capture, appears in the cold fusion reactions. The nature of this phenomenon is connected by the PES ($U(Z, R)$) landscape which is used to estimate the complete fusion probability in competition with quasifission. In Fig. 2, the capture stage path is shown by arrow (a) and complete fusion by multinucleon transfer occurs (b) if system overcomes intrinsic fusion barrier. Arrow (c) shows one of possibilities of the DNS quasifission from its more charge symmetric configurations.

PES is calculated as a sum of the reaction energy balance (Q_{gg}) and the nucleus-nucleus potential ($V(R)$) between interacting nuclei:

$$U(Z, A, \ell, R) = Q_{\text{gg}} + V(Z, A, \ell, R), \quad (2)$$

where $Z = Z_1$ and $A = A_1$ are charge and mass numbers of a nucleus of the DNS while the ones of another nucleus are $Z_2 = Z_{\text{tot}} - Z$ and $A_2 = A_{\text{tot}} - A$, where Z_{tot} and A_{tot} are the total charge and mass numbers of a reaction, respectively.

The driving potential $U_{\text{dr}}(Z, R_m)$ is shown by the broken dot-dashed line in Fig. 2 and it is determined by the minimum values of the potential wells for each charge value Z . The position

of the minimum value of interaction potential on the relative distance is denoted as R_m . The values of $U_{dr}(Z, R_m)$ as a function of angular momentum ℓ are found from the data of PES calculated by formula

$$U_{dr}(Z, A, \ell, R_m) = Q_{gg} + V(Z, A, \ell, R_m). \quad (3)$$

If there is no potential well of $V(Z, A, \ell, R)$ at a given value of angular momentum or for symmetric massive nuclei, we use R_m corresponding to the smallest value of the derivation $|\partial V(Z, A, \ell, R_m)/\partial R|$ in the contact area of nuclei.

In Fig. 3 we compare the driving potentials calculated for the systems formed in the $^{48}\text{Ca}+^{248}\text{Cm}$ and $^{58}\text{Fe}+^{232}\text{Th}$ reactions which can lead to the CN formation with ^{296}Lv and ^{290}Lv , respectively, as a function of the fragment charge number. PES and driving potential U_{dr} are functions of the orientation angles α_1 and α_2 of axial symmetry axes of interacting nuclei. The results reported in figures 5-7, 14 and 15 have been obtained for the orientation angles $\alpha_1 = 45^\circ$ and $\alpha_2 = 60^\circ$.

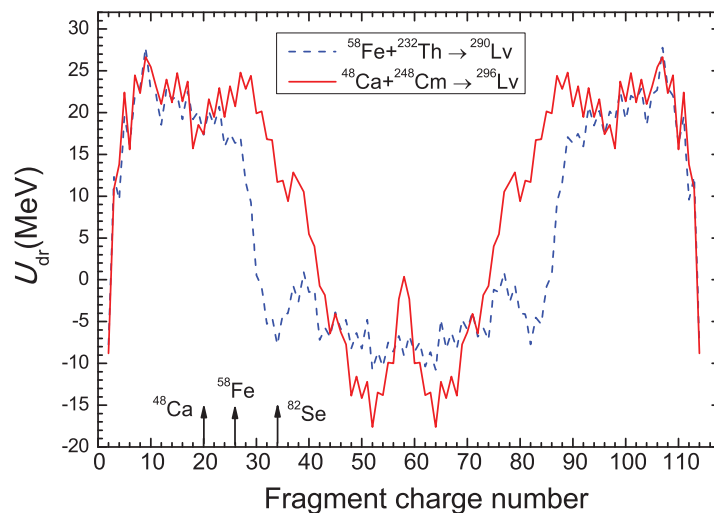


Figure 3. (Color online) Comparison of the driving potentials calculated for the systems formed in the $^{48}\text{Ca}+^{248}\text{Cm}$ and $^{58}\text{Fe}+^{232}\text{Th}$ reactions which can lead to formation of isotopes $A=296$ and 290 of the superheavy element Lv ($Z=116$), respectively, as a function of a fragment charge number.

It is seen from Fig. 3 that the driving potential decreases abruptly for the fragment with charge number larger than $Z = 30$ for both the $^{48}\text{Ca}+^{248}\text{Cm}$ and $^{58}\text{Fe} + ^{232}\text{Th}$ reactions. If the value of the driving potential corresponding to the entrance channel is very low in respect to its maximum value in the fusion direction $Z \rightarrow 0$, the intrinsic fusion barrier B_{fus}^* becomes larger and the hindrance to complete fusion will be very strong. The method of calculating $B_{fus}^*(Z, A, \ell)$ is shown in Fig. 4. It is determined as a difference between the maximum value of the driving potential between $Z = 0$ and $Z = Z_P$ and its value corresponding to the initial charge value:

$$B_{fus}^* = U_{dr}^{\max} - U_{dr}(Z_P), \quad (4)$$

where is $U_{dr}^{\max} = U_{dr}(Z = 9)$; while are $Z_P = 20$ and $Z_P = 26$ for the reactions with ^{48}Ca and ^{58}Fe , respectively. The values of B_{fus}^* are equal to 8.5 MeV and 11.5 MeV for the $^{48}\text{Ca}+^{248}\text{Cm}$ and $^{58}\text{Fe}+^{232}\text{Th}$ reactions, respectively (see Fig. 3). If we consider for example the $^{82}\text{Se}+^{208}\text{Pb}$

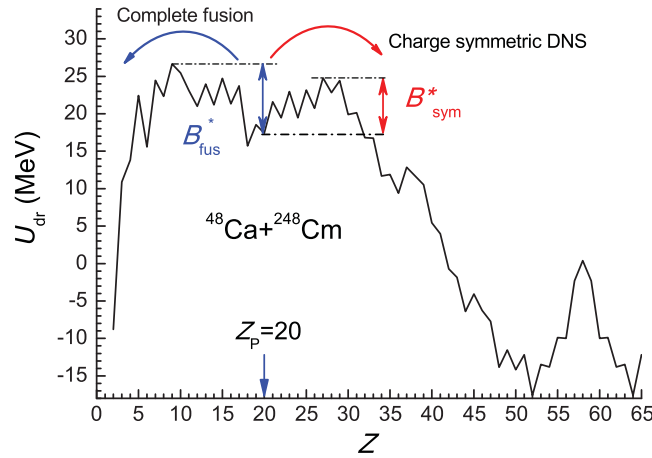


Figure 4. (Color online) Intrinsic fusion barrier B_{fus}^* and intrinsic barrier B_{sym}^* against to symmetry configurations from the initial charge asymmetry $Z=20$ on the driving potential (solid line) for the $^{48}\text{Ca}+^{248}\text{Cm}$ reaction.

$\rightarrow^{290}\text{Lv}$ cold fusion reaction where Z_p is equal to 34, such a reaction is strongly hopeless of reaching complete fusion since $B_{\text{fus}}^*=34$ MeV (please check if this value is correct).

The hindrance to evolution of DNS in direction of the symmetric charge distributions is determined by the barrier B_{sym}^* which is determined by the similar way as in the case of B_{fus}^* but the maximum value of the driving potential from symmetric charge region is used (see Fig. 4).

The study of dynamics of the heavy ion collisions near the Coulomb barrier energies showed that complete fusion does not occur immediately in the case of massive nucleus collisions [13–17]. In Ref. [18], authors estimated the excitation functions of the ER formation in the $^{50}\text{Ti}+^{249}\text{Bk}$ and $^{50}\text{Ti}+^{249,252}\text{Cf}$ reactions by using a newly developed DNS model with a dynamical potential energy surface. The authors concluded that taking into account dynamical deformation of DNS fragments, the calculation by this model leads to a decrease of the fusion probability and, consequently, to a decrease of the ER formation cross section.

The evolution of DNS may end with the CN formation with excitation energy E_{CN}^* in the statistically equilibrated state or it may lead to formation of two fragments without reaching the CN state. The latter process is quasifission. It takes place when DNS prefers to break down into two fragments instead of being transformed into fully equilibrated CN. The quasifission products may have characteristics similar to ones of fusion-fission products. For example, the total kinetic energy of the quasifission fragments is close to that of fission fragments. The mass and angular distributions of the fragments depend on the entrance channel properties and may overlap, causing difficulties in identification of a mechanism which produces the corresponding reaction products [19,20]. We should stress the dominant role of the quasifission channel in the cold fusion reactions that causes strong hindrance to the formation of CN during the evolution of DNS.

The mononucleus survived to quasifission can reach the equilibrium shape, and it may be transformed into CN. In this case, it is important to know how large is the angular momentum L_{MN} of mononucleus for its transformation to the equilibrated state of CN since the fission barrier B_f of a being formed CN depends on its angular momentum. The macroscopic fission barrier $B_f(L)$ of the rotating nucleus disappears at large values of $L_{\text{MN}} > L_f$ [21] and the mononucleus undergoes to fast fission leading to formation of two fragments similar to that

from fusion-fission or quasifission. So, fast fission is splitting of mononucleus before reaching equilibrated CN if $L_{CN} > L_f$. We remain that quasifission process can occur at all values of L_{DNS} of DNS. This is one of main differences between fast fission and quasifission; the other difference is that the fast fission process is the decay of the non-equilibrated complete fusion system, while the quasifission process is the decay of the excited DNS without to reach the stage of complete fusion.

The heated and rotating CN must survive against fission to be registered by detector as the recoil nucleus by emission of mainly neutrons, protons, α -particles, and gamma-quanta. The fusion-fission channel can be enriched by the fast fission products and both processes are characterized by the properties of the fission barrier described by the liquid drop model for the intermediate mass and heavy nuclei. For the very massive nuclei the properties of fission barrier is connected by the shell corrections which is determined by the microscopic models. This last contribution is decisive for the stability of very heavy atomic nuclei with charge number $Z > 106$ against fission because the contribution to the fission barrier due to the liquid drop model is disappeared. So, the possible existence of some value for the fission barrier may be due to the contribution of shell effects in the binding energy [22], which is sensitive to the L and E_{CN}^* values. Therefore, fission barrier of nucleus related with both nature (liquid drop and shell effect) disappears at large values of angular momentum L [21] and when shell effects have been completely damped [23] as a function of the excitation energy and angular momentum. Consequently, a mononucleus, which has survived against quasifission, can not reach CN equilibrium shape and suffers fast fission. Finally, the CN, which survived against fission by emission of particles during its cooling, forms the ER which can be registered as a superheavy element.

The main scope of this work is to reproduce the measured data for the superheavy elements with $Z = 116$ and $Z = 118$ formed in the $^{48}\text{Ca}+^{248}\text{Cm}$ and $^{48}\text{Ca}+^{249}\text{Cf}$ reactions, respectively, and to make predictions for σ_{ER} in the $^{58}\text{Fe}+^{232}\text{Th}$ and $^{64}\text{Ni}+^{232}\text{Th}$ reactions which can be used in future experiments.

2.1. Capture and fusion cross section in collisions of deformed nuclei

The final results of the partial capture and complete fusion cross sections are obtained by averaging the contributions from the different orientation angles α_1 and α_2 (relatively to the beam direction) of the projectile and target nuclei, respectively [17]:

$$\langle \sigma_{fus}(E_{c.m.}, \ell) \rangle = \int_0^{\pi/2} \sin \alpha_1 \int_0^{\pi/2} \sigma_{fus}(E_{c.m.}, \ell; \alpha_1, \alpha_2) \sin \alpha_2 d\alpha_1 d\alpha_2. \quad (5)$$

The partial fusion cross section $\sigma_{fus}(E_{c.m.}, \ell; \alpha_1, \alpha_2)$ is determined by the product of the partial capture cross section $\sigma_{cap}(E_{c.m.}, \ell; \alpha_1, \alpha_2)$ and probability P_{CN} of the transformation of DNS into CN:

$$\sigma_{fus}(E, \ell; \alpha_1, \alpha_2) = \sigma_{cap}(E, \ell; \alpha_1, \alpha_2) P_{CN}(E, \ell; \alpha_1, \alpha_2). \quad (6)$$

The calculations of capture and fusion cross sections were performed in the framework of the DNS model. The capture probability and the largest value of orbital angular momentum (ℓ_d), leading to capture at the given values of the orientation angles α_1 and α_2 , are calculated by solving equations of the relative motion of nuclei and orbital angular momentum of collision [16,17,19,24]. As a result we have partial capture cross sections (angular momentum distribution of DNS) for a given value of the collision energy $E_{c.m.}$. Certainly, partial capture cross section is equivalent to cross section of formation of DNS with given angular momentum L_{DNS} and excitation energy E_Z^* .

The excitation energy E_Z^* of interacting nuclei of DNS at given collision energy $E_{c.m.}$ and orbital angular momentum ℓ is calculated by taking into account the changes of the mass and

charge numbers from the initial values A_P and Z_P for projectile (A_T and Z_T for target-nucleus) to the current values A and Z :

$$E_Z^*(A, \ell; \alpha_1, \alpha_2) = E_{c.m.} - V(Z, A, \ell, R_m; \alpha_1, \alpha_2) + \Delta Q_{gg}(Z, A). \quad (7)$$

Here $\Delta Q_{gg}(Z, A)$ is the change of binding energies of the DNS nuclei due to nucleon transfer between nuclei:

$$\Delta Q_{gg}(Z, A) = B_Z(A) + B_{Z_{tot}-Z}(A_{tot} - A) - (B_{Z_P}(A_P) + B_{Z_T}(A_T)), \quad (8)$$

where $Z_{tot} = Z_P + Z_T$ and $A_{tot} = A_P + A_T$;

$V(Z, A, \ell, R_m; \alpha_1, \alpha_2)$ is the minimum value of potential well in the nucleus-nucleus interaction.

During evolution of DNS an intense mass transfer takes place and, in dependence on the landscape of potential energy surface and entrance channel, the mass asymmetry degree of freedom may be fully or partially equilibrated [25]. The duration of the quasifission is one order of magnitude larger than the time which is needed to reach the thermal equilibrium. It is more than $5 \cdot 10^{-21}$ s which was estimated by the analysis of experimental data on quasifission reactions [26, 28, 29]. The validity of using of the statistical method is righteous due to the fact that a full relaxation of the relative kinetic energy and mass (charge) asymmetry between the two fragments takes place at quasifission process [30].

Therefore, while DNS exists, we have an ensemble $\{Z\}$ of the DNS configurations which contributes to the competition between complete fusion and quasifission with probabilities $\{Y_Z\}$. The dependence of barrier B_{fus}^* and excitation energy of DNS E_Z^* for given charge Z and mass asymmetry A on angular momentum and orientation angles α_i ($i=1,2$) of the symmetry axis of interacting nuclei is connected with the method of calculation of the interacting potential between nuclei of DNS which is sensitive to those variables. Consequently, the fusion factor P_{CN} for the given reaction depends on the same variables through the charge distribution $Y_Z(E_Z^*)$ and fusion factor $P_{CN}^{(Z)}$ from charge asymmetry configuration Z :

$$P_{CN}(E_Z^*, \ell; \alpha_1, \alpha_2) = \sum_{Z_{sym}}^{Z_{max}} Y_Z(E_Z^*, \ell) P_{CN}^{(Z)}(E_Z^*, \ell; \alpha_1, \alpha_2), \quad (9)$$

where $P_{CN}^{(Z)}(E_Z^*, \ell; \alpha_1, \alpha_2)$ is the fusion probability for DNS having excitation energy E_Z^* at charge asymmetry Z and orientation angles of symmetry axis of its fragments are equal to α_1 and α_2 . The evolution of Y_Z is calculated by solving the transport master equation. The details of calculations of $P_{CN}^{(Z)}(E_Z^*, \ell; \alpha_1, \alpha_2)$ can be found in Refs. [16, 17, 19, 24].

2.2. Quasifission and fast fission of mononucleus evolving to equilibrium shape of compound nucleus

Another binary process which leads to the formation of two fragments similar to that from fusion-fission or quasifission is the fast fission. The fast fission occurs only at large values of angular momentum $\ell > \ell_f$ causing disappearance of the macroscopic fission barrier $B_f(\ell)$ of the rotating nucleus [21].

The partial cross section of fast fission is determined as cross section fusion with $\ell > \ell_f$ because mononucleus has survived against quasifission. The fast fission cross section is calculated by summing the contributions of the partial waves corresponding to the range $\ell_f \leq \ell \leq \ell_d$ leading to the formation of the mononucleus:

$$\sigma_{ff}(E_{c.m.}; \beta_P, \alpha_2) = \sum_{\ell_f}^{\ell_d} (2\ell + 1) \sigma_{cap}(E_{c.m.}, \ell; \beta_P, \alpha_2) P_{CN}(E_{c.m.}, \ell; \beta_P, \alpha_2). \quad (10)$$

The capture cross section in the framework of the DNS model is equal to the sum of the quasifission, fusion, and fast fission cross sections:

$$\sigma_{\text{cap}}(E_{\text{c.m.}}; \beta_1, \alpha_2) = \sigma_{\text{qf}}(E_{\text{c.m.}}; \beta_1, \alpha_2) + \sigma_{\text{fus}}(E_{\text{c.m.}}; \beta_1, \alpha_2) + \sigma_{\text{ff}}(E_{\text{c.m.}}; \beta_1, \alpha_2). \quad (11)$$

It is clear that the fusion cross section includes the cross sections of ERs and fusion-fission products. Obviously, the quasifission cross section is defined by

$$\sigma_{\text{qf}}(E_{\text{c.m.}}; \beta_P, \alpha_2) = \sum_{\ell=\ell_f}^{\ell_d} (2\ell+1) \sigma_{\text{cap}}(E_{\text{c.m.}}, \ell; \beta_P, \alpha_2) (1 - P_{\text{CN}}(E_{\text{c.m.}}, \ell; \beta_P, \alpha_2)), \quad (12)$$

i.e. the quasifission process can take place in the whole range of the orbital angular momentum values leading to capture, including central collisions ($\ell = 0$). This is important conclusion since the separation of the ranges of the angular momentum corresponding to the fusion-fission and quasifission products by some critical value ℓ_{cr} in the analysis of the angular distribution of the fissionlike products is doubtful. The results of our calculations show that the ranges of the quasifission and fusion-fission overlap.

3. Comparison of the $^{48}\text{Ca}+^{248}\text{Cm}$ and $^{58}\text{Fe}+^{232}\text{Th}$ reactions leading to superheavy element Lv

The importance of the charge asymmetry in the CN formation is seen from the comparison of the $^{48}\text{Ca}+^{248}\text{Cm}$ and $^{58}\text{Fe}+^{232}\text{Th}$ reactions leading to the ^{296}Lv and ^{290}Lv CN, respectively. Fusion excitation functions, which have been obtained for these reactions, are presented by solid line in Figs. 5 and 6, respectively. We stress two main differences: 1) the cross section of the CN formation is larger in the reaction with ^{48}Ca in comparison with the $^{58}\text{Fe}+^{232}\text{Th}$ reaction; 2) CN formed in the former reaction has smaller excitation energy.

In Figs. 5 and 6, capture and quasifission cross sections are nearly equal to each other due to the dominant contribution of the quasifission cross section to capture in comparison with the sum of the fast fission and compound nucleus formation cross sections.

The number of events going to quasifission increases drastically with the increasing Coulomb interaction and rotational energy in the entrance channel [27, 31]. The advantage of the $^{48}\text{Ca}+^{248}\text{Cm}$ in synthesis of superheavy element is seen already in the CN formation stage.

One can see in Fig. 6 that the fusion excitation function decreases strongly at low energies $E_{\text{c.m.}} < 250$ MeV. This effect is connected with the increase of hindrance to fusion since at these low energies the collisions with small orientation angles (α_1 -projectile and α_2 -target) can only contribute to the CN formation [17, 32]. Collisions with larger orientation angles α_1 and α_2 can not lead to capture since the collision energy in the center-of-mass system is not enough to overcome the Coulomb barrier of the entrance channel. For the DNS formed in collisions with small orientation angles α_1 and α_2 , the intrinsic fusion barrier B_{fus}^* is large [17]. So, the hindrance to complete fusion depends on the orientation angles: more elongated shape of the DNS formed at collisions with small orientation angles (tip-to-tip configurations) promotes the quasifission rather than the formation of the CN [17, 32].

Theoretical results of the ER cross sections for the synthesis of the element $Z = 116$ are compared with the experimental data in Fig. 7. In this figure, the full triangles and squares show experimental data of the ER cross sections measured in 3n- and 4n-channels, respectively, in the $^{48}\text{Ca}+^{248}\text{Cm}$ reaction [2]; the curves show theoretical results obtained in this work for the 2n-(dot-dashed line), 3n-(dashed line), 4n-(solid line), and 5n-channel (dotted line) by the DNS and advanced statistical models [33, 34] using the mass tables of Möller and Nix [11] (thin lines) and of Muntian *et al.* [12] (thick lines).

The mass values of the Warsaw group [12] are larger than ones of Möller and Nix [11] by 2-3 MeV for the isotopes of superheavy nuclei with $Z > 110$ and fission barriers [6, 7] are

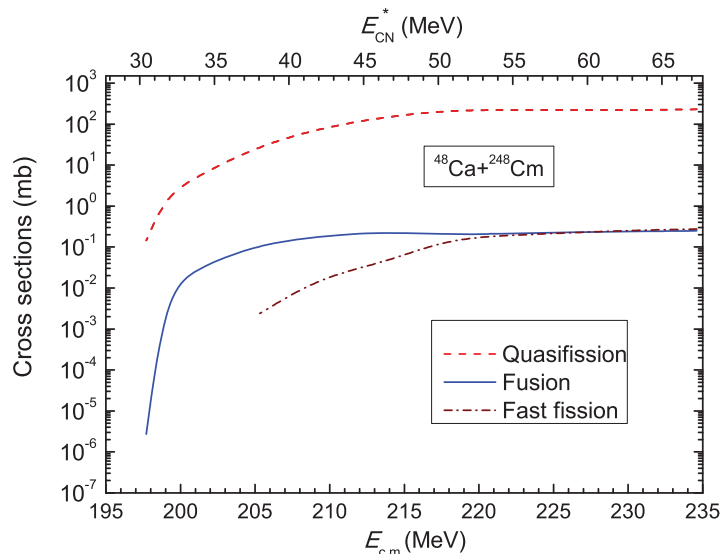


Figure 5. (Color online) (Color online) Quasifission (dashed line), complete fusion (solid line) and fast fission (dot-dashed line) excitation functions calculated by the DNS model [17, 24, 31] for the $^{48}\text{Ca}+^{248}\text{Cm}$ reaction leading to formation of the ^{296}Lv CN. The excitation energy E_{CN}^* (top axis) is calculated by the use of the Möller and Nix mass table [11].

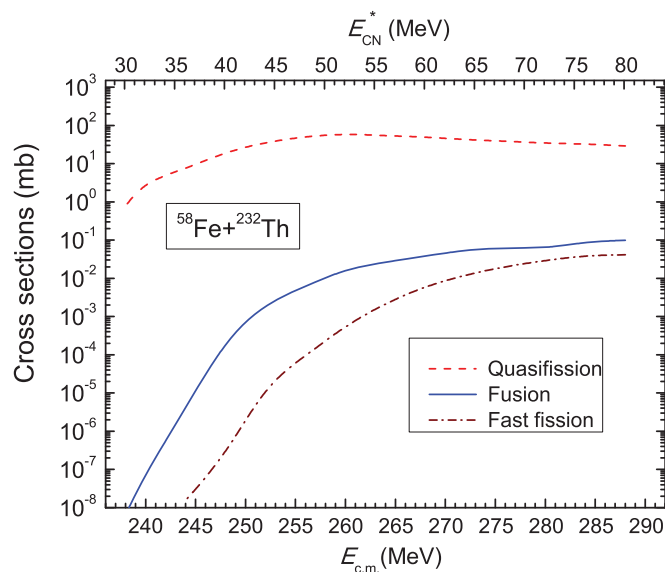


Figure 6. (Color online) As Fig. 5 but for the $^{58}\text{Fe}+^{232}\text{Th}$ reaction leading to formation of the ^{290}Lv .

smaller by 2-3 MeV in comparison with the similar values of Möller and Nix [11]. As a result, the Warsaw group results lead to two main consequences: 1) the excitation energy of the CN ($E_{\text{CN}}^* = E_{\text{c.m.}} + Q_{\text{gg}} - V_{\text{rot}}$) will be lower since the absolute value of $Q_{\text{gg}} = B_{\text{proj}} + B_{\text{targ}} - B_{\text{CN}}$ (negative) is larger; 2) the fission probability will be large in comparison with the case of using fission barrier of the Möller and Nix [11] model. When the binding energies and fission barriers of the Warsaw group [12] are used, the total score is that the survival probability W_{sur} becomes

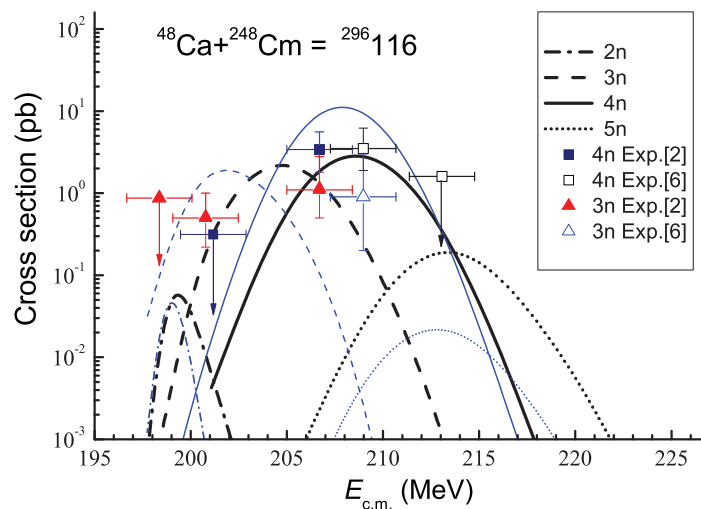


Figure 7. (Color online) Comparison between the ER excitation functions for the $^{48}\text{Ca}+^{248}\text{Cm}$ reaction calculated by using mass tables of Möller and Nix [11] (thin lines) and of the Warsaw group [12] (thick lines) for the 2n (dot-dashed lines), 3n (dashed lines), 4n (solid lines), and 5n (dotted lines) channels calculated by the advanced statistical model [33, 34]. The experimental data corresponding to the 3n (triangles) and 4n (squares) channels are obtained from Refs. [1, 2] (filled symbols) and [5] (open symbols).

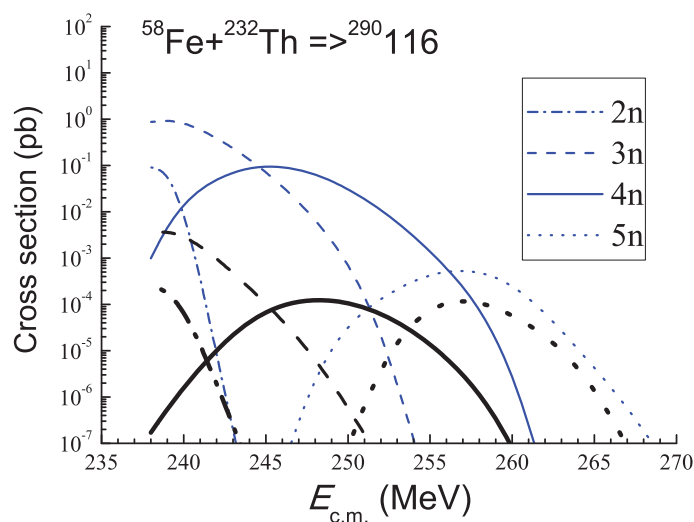


Figure 8. (Color online) As Fig. 7 but for the $^{58}\text{Fe}+^{232}\text{Th}$ reaction.

smaller in comparison with the case of using fission barrier of the Möller and Nix [11] model.

The results of σ_{ER} for the $^{48}\text{Ca}+^{248}\text{Cm}$ reaction, calculated by the use of the mass tables of the Warsaw group, better describe the experimental data than the ones obtained by using Möller *et al.* The largest cross section of the yield of superheavy element corresponds to the 4n-channel is about 10 pb when the collision energy is in the range $E_{\text{c.m.}}=205\text{--}212$ MeV (thin

solid line in Fig. 7).

Concerning the ER formation in the more symmetric $^{58}\text{Fe}+^{232}\text{Th}$ reaction, the results indicate that this reaction is less favorable in comparison with the $^{48}\text{Ca}+^{248}\text{Cm}$ reaction to be used in the synthesis of superheavy element $Z = 116$. The largest cross section for the 3n-channel is about 1 pb (see Fig. 8) if we use the mass tables of Möller and Nix [11] (thin dashed lines), while the use of the mass table and fission barriers of the Warsaw group leads to the two orders of magnitude lower cross section (thick dashed line) in comparison with the one in case of the using the mass tables of Möller and Nix.

4. Comparison of $^{48}\text{Ca}+^{249}\text{Cf}$ and $^{64}\text{Ni}+^{232}\text{Th}$ reactions leading to superheavy element $Z=118$

The capture, quasifission, fusion, and fast fission cross sections calculated in this work for the $^{48}\text{Ca}+^{249}\text{Cf}$ and $^{64}\text{Ni}+^{232}\text{Th}$ reactions are presented in Figs. 9 and 10, respectively.

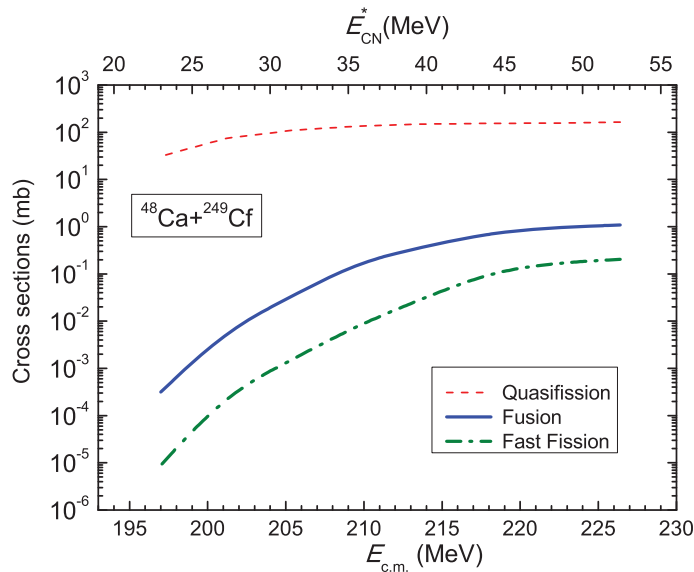


Figure 9. (Color online) As Fig. 5 but for the $^{48}\text{Ca}+^{249}\text{Cf}$ reaction leading to formation of the $^{297}118$ CN.

The comparison between these figures shows that, at low energies, the capture cross section in the $^{64}\text{Ni}+^{232}\text{Th}$ reaction is much smaller than that in the $^{48}\text{Ca}+^{249}\text{Cf}$ reaction. The curve of capture cross section for the $^{64}\text{Ni}+^{232}\text{Th}$ reaction goes down at larger energies $E_{\text{c.m.}} > 263$ MeV. But fusion cross section is very small due to drastic hindrance to complete fusion since at low energies only collisions with small values of orientation angles α_2 lead to the capture, *i.e.* to formation of the long living DNS. The latter formed in collisions with small values of α_2 has large intrinsic barrier B_{fus}^* (see Fig. 11) and small quasifission barrier B_{qf} for this reaction in comparison with $^{48}\text{Ca}+^{249}\text{Cf}$ (see Fig. 12). This means that the potential well in the nucleus-nucleus interaction is shallow since the Coulomb interaction is stronger for more symmetric reactions ($z = 248.41$ for $^{64}\text{Ni}+^{232}\text{Th}$ reaction). These two reasons, which are unfavorable for complete fusion [17], lead small fusion probability for the $^{64}\text{Ni}+^{232}\text{Th}$ reaction at low energies.

The advantage of the charge asymmetric system (hot fusion reaction) in complete fusion appears at the second stage of the reaction mechanism leading to the CN formation: the intrinsic fusion barrier B_{fus}^* decreases and quasifission barrier B_{qf} increases with increasing the DNS charge asymmetry (see Fig. 4).

The theoretical ER excitation functions of different neutron-emission channels for these two systems are presented in Figs. 13 and 14. In each of the figures the ER cross sections are obtained

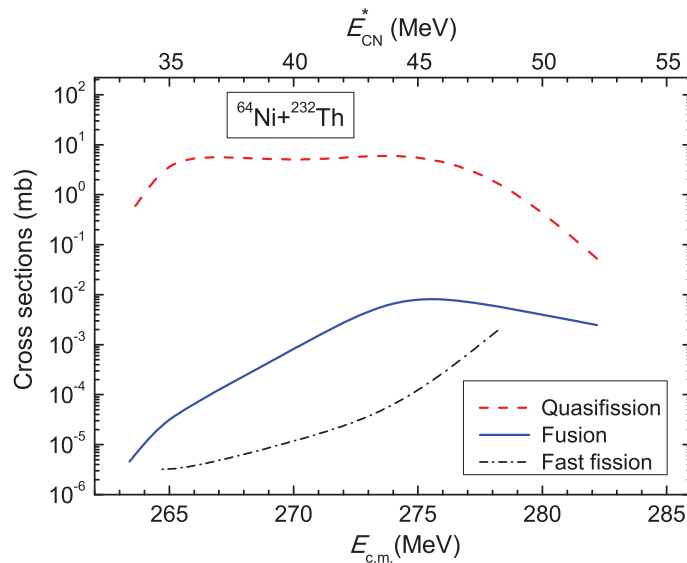


Figure 10. (Color online) Same as Fig. 5 but for the $^{64}\text{Ni}+^{232}\text{Th}$ reaction which could lead to formation of the $^{296}118$ CN.

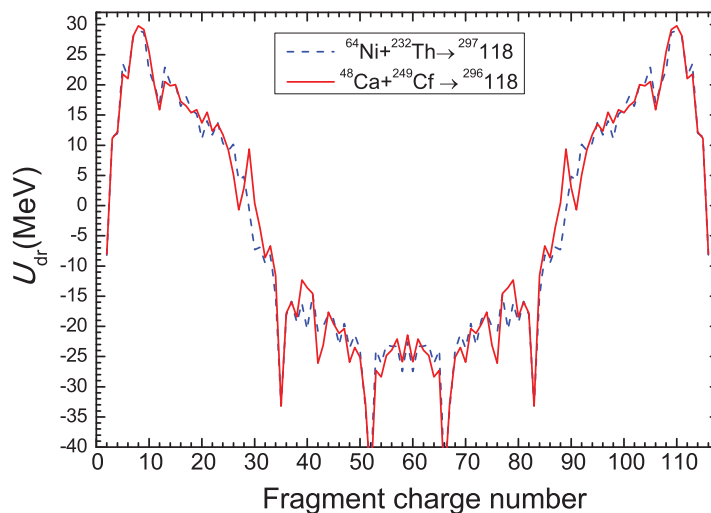


Figure 11. (Color online) Comparison of the driving potentials calculated for the DNS formed in the $^{48}\text{Ca}+^{249}\text{Cf}$ and $^{64}\text{Ni}+^{232}\text{Th}$ reactions which can lead to formation of isotopes $A=297$ and 296 of the superheavy element $Z=118$ as a function of the fragment charge number.

by using binding energies and fission barriers calculated in the microscopic-macroscopic models of Möller and Nix [11] and of the Warsaw group [12] are compared.

In Figs. 13 and 14, the results calculated for the $^{48}\text{Ca}+^{249}\text{Cf}$ reaction [23] leading to $^{297}118$ CN and for the $^{64}\text{Ni}+^{232}\text{Th}$ reaction leading to the same superheavy element $^{296}118$ with smaller mass number, respectively, are presented. In Fig. 13, the experimental data [2] corresponding to the synthesis of SHE $^{294}118$ after emission of three neutrons from the $^{297}118$ CN are shown by squares.

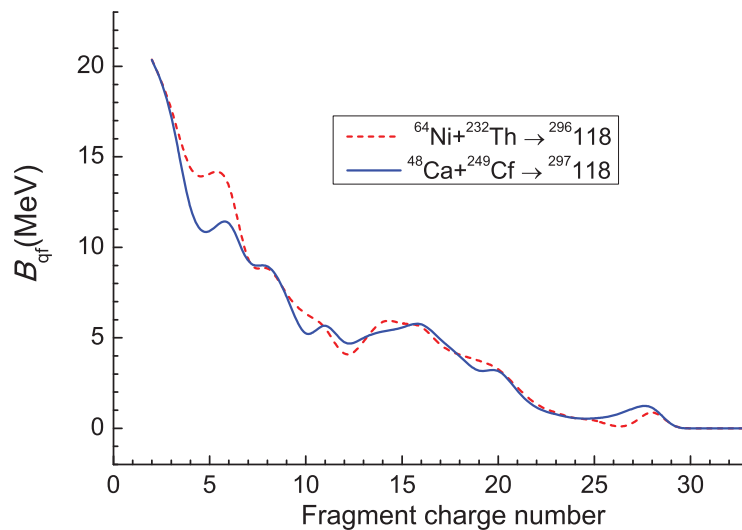


Figure 12. (Color online) The quasifission barriers of the DNS fragments as a function of their charge numbers for the $^{48}\text{Ca}+^{249}\text{Cf}$ (solid curve) and $^{64}\text{Ni}+^{232}\text{Th}$ (dashed curve) reactions.

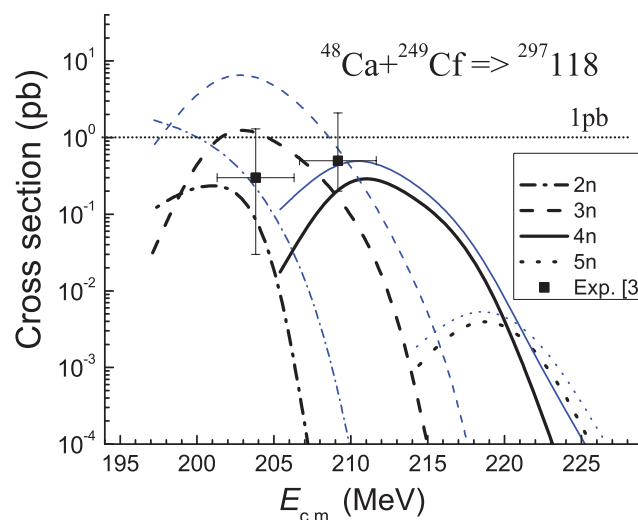


Figure 13. (Color online) Comparison between the ER excitation functions for the $^{48}\text{Ca}+^{249}\text{Cf}$ reaction calculated by using mass tables of Möller and Nix [11] (thin lines) and of the Warsaw group [12] (thick lines) for the 2n (dot-dashed lines), 3n (dashed lines), 4n (solid lines), and 5n (dotted lines) channels calculated by the advanced statistical model [33, 34]. The experimental data of the 3n channel from Ref. [2] are presented by squares.

One can see from Fig. 14 that the results obtained for all xn -channels of ER formation in the $^{64}\text{Ni}+^{232}\text{Th}$ reaction are very small. The largest point of the 4n-channel curve is about 10 fb (thin solid line) in the case when we used masses of the Möller and Nix table [11] in our calculations. The use of the masses obtained by the Warsaw group [12] leads to the ER cross sections (thick lines) which are more lower than ones obtained in the former case.

The ER cross sections of the 4n and 5n channels for the $^{64}\text{Ni}+^{232}\text{Th}$ reaction obtained by

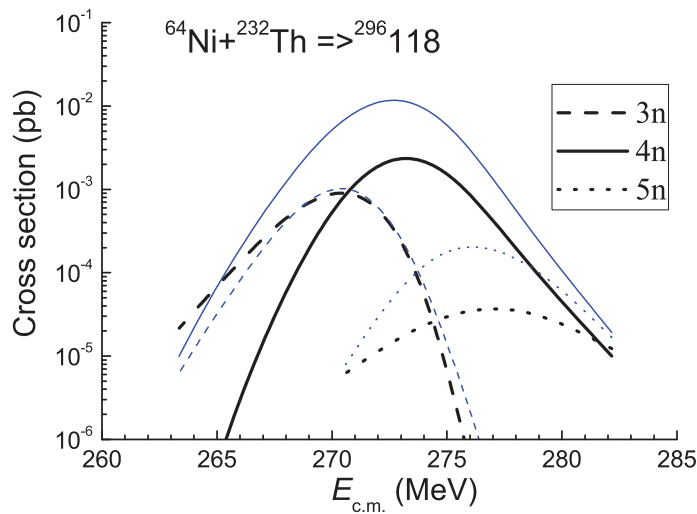


Figure 14. (Color online) As Fig. 13 but for the $^{64}\text{Ni}+^{232}\text{Th}$ reaction.

the using masses of the Möller and Nix table [11] are larger than those calculated by the using mass tables of Warsaw group [12], while the same behaviour does not appear by an evident way for the 3n channel. This is due to the effect of the different E_{CN}^* threshold values for the 3n channel when the masses of table [11] and Warsaw group [12] are considered. In the first case, the threshold energy for the 3n channel is at the $E_{\text{CN}}^* = 35$ MeV, while for the second case it is at $E_{\text{CN}}^* \equiv 30.5$ MeV. Due to the above-mentioned conditions for the $^{64}\text{Ni}+^{232}\text{Th}$ reaction, the excitation function of the 3n channel is strongly different in comparison with the ones shown in Fig. 14 for the 4n and 5n channels.

5. Conclusions

In the framework of the combined DNS and advanced statistical models, the ER excitation functions for the $^{48}\text{Ca}+^{248}\text{Cm}$ and $^{58}\text{Fe}+^{232}\text{Th}$ reactions leading to the superheavy element Lv ($Z=116$) and the $^{48}\text{Ca}+^{249}\text{Cf}$ and $^{64}\text{Ni}+^{232}\text{Th}$ reactions leading to the superheavy element $Z=118$ have been calculated. The ER cross sections of the 3n- and 4n-channels for the $^{48}\text{Ca}+^{248}\text{Cm}$ reaction presented Refs. [1, 2] are well described when the Warsaw group mass tables [12] are used, while in both cases the use of the Möller and Nix [11] mass tables leads to overestimation of the experimental data.

The theoretical values of ER cross sections for the $^{48}\text{Ca}+^{249}\text{Cf}$ reactions (Fig. 13) are in good agreement with the experimental data presented in Ref. [1, 2] when we use the mass table and fission barriers of Warsaw group.

The results of the ER excitation functions for the $^{58}\text{Fe}+^{232}\text{Th}$ reaction indicate that this reaction is less favorable to be used in the synthesis of superheavy element $Z = 116$. The strong hindrance at low energies is caused by the large intrinsic fusion barrier B_{fus}^* for the small orientation angles of the symmetry axis of the deformed projectile ^{58}Fe ($\beta_2 = 0.2$) and target ^{232}Th ($\beta_2 = 0.26$) nuclei. Therefore, the curve of the fusion excitation function increases slightly with the increasing beam energy. The largest cross section for the 3n-channel is about 1 pb (see Fig. 8), if we use the mass tables of Möller and Nix [11] (thin dashed line), while the use of the mass table and fission barriers of Warsaw group leads to much lower cross sections (thick dashed line), no more than 40 fb.

The results obtained for all xn -channels of ER formation in the $^{64}\text{Ni}+^{232}\text{Th}$ reaction are very small (see Fig. 14). The largest point of the $4n$ -channel curve is about 10 fb (thin solid line) when masses from the Möller and Nix table [11] were used in our calculations. The use of the Warsaw group mass tables [12] leads to values of the ER cross sections, which are sufficiently lower than ones of the former case. That means this reaction is not favorable to observe an event corresponding to the synthesis of any isotopes of the superheavy element 118.

5.1. Acknowledgments

A. K. Nasirov is grateful to the Rare Isotope Science Project of the Institute for Basic Science of the Republic of Korea for the support the collaboration between the Dubna and Daejeon groups, and he thanks the Russian Foundation for Basic Research and Fondazione Bonino-Pulejo for the partial financial support in the performance of this work. The work of Y. Kim and K. Kim was supported by the Rare Isotope Science Project funded by the Ministry of Science, ICT and Future Planning (MSIP) and National Research Foundation (NRF) of Korea.

References

- [1] Yu.Ts. Oganessian *et al.*, Phys. Rev. C **70**, 064609 (2004).
- [2] Yu.Ts. Oganessian *et al.*, Phys. Rev. C **74**, 044602 (2006).
- [3] L. Stavsetra *et al.*, Phys. Rev. Lett. **103**, 132502 (2009).
- [4] J.M. Gates *et al.*, Phys. Rev. C **83**, 054618 (2011).
- [5] S. Hofmann *et al.*, Eur. Phys. J. A **48**, 62 (2012).
- [6] M. Kowal, P. Jachimowicz, A. Sobiczewski, Phys. Rev. C **82**, 014303 (2010).
- [7] M. Kowal and A. Sobiczewski, Int. J. Mod. Phys. E **18**, 914 (2009).
- [8] S. Hofmann, Rep. Prog. Phys. **61**, 639 (1998).
- [9] K. Morita *et al.*, Jour. Phys. Soc. Japan, **81**, 103201 (2012).
- [10] G. Audi, A.H. Wapstra, Nucl. Phys. **A595**, 509 (1995).
- [11] P. Möller and J.R. Nix, J. Phys. G: Nucl. Part. Phys. **20**, 1681 (1994).
- [12] I. Muntian, Z. Patyk, A. Sobiczewski, Phys. At. Nuclei **66**, 1015 (2003).
- [13] B.B. Back *et al.*, Phys. Rev. C **32**, 195 (1985).
- [14] N.V. Antonenko *et al.*, Phys. Rev. C **51**, 2635 (1995).
- [15] G.G. Adamian, N.V. Antonenko, W. Scheid, Phys. Rev. C **68**, 034601 (2003).
- [16] G. Fazio *et al.*, Eur. Phys. J. A **19**, 89 (2004).
- [17] A.K. Nasirov *et al.*, Nucl. Phys. A **759**, 342 (2005).
- [18] N. Wang, E.G. Zhao, W. Scheid, Sh.G. Zhou, Phys. Rev. C **85**, 041601(R) (2012).
- [19] A.K. Nasirov *et al.*, Phys. Rev. C **79**, 024606 (2009).
- [20] A.K. Nasirov *et al.*, Int. Jour. of Mod. Phys. E, **18**, 841 (2009).
- [21] A.J. Sierk, Phys. Rev. C **33**, 2039 (1986).
- [22] A. Sobiczewski, K. Pomorski, Prog. Part. Nucl. Phys. **58**, 292 (2007).
- [23] G. Mandaglio, G. Giardina, A.K. Nasirov, A. Sobiczewski, Phys. Rev. C **86**, 064607 (2012).
- [24] G. Fazio *et al.*, Mod. Phys. Lett. A **20**, 391 (2005).
- [25] R. Bock *et al.*, Nucl. Phys. A **388**, 334 (1982).
- [26] J. Töke *et al.*, Nucl. Phys. **A440**, 327 (1985).
- [27] G. Giardina, S. Hofmann, A.I. Muminov, A.K. Nasirov, Eur. Phys. J. A **8**, 205 (2000).
- [28] D.J. Hinde *et al.*, Phys. Rev. C **45**, 1229 (1992).
- [29] K. Siwek-Wilczynska, J. Wilczynski, R. H. Siemssen, H. W. Wilschut, Phys. Rev. C **51**, 2054 (1995).
- [30] B.B. Back *et al.*, Phys. Rev. C **53**, 1734 (1996).
- [31] G. Fazio *et al.*, Phys. Rev. C **72**, 064614 (2005).
- [32] D.J. Hinde *et al.*, Phys. Rev. Lett. **74**, 1295 (1995).
- [33] A. D'Arrigo, G. Giardina, M. Herman, A. Taccone, Phys. Rev. C **46**, 1437 (1992).
- [34] R.N. Sagaidak *et al.*, J. Phys. G **24**, 611 (1998).